

# In Quest of Ground Truth: Learning Confident Models and Estimating Uncertainty in the Presence of Annotator Noise

Asma Ahmed Hashmi

Artem Agafonov

Aigerim Zhumabayeva

Mohammad Yaqub

Martin Takáč

Mohamed bin Zayed University of Artificial Intelligence (MBZUAI)

Masdar City, Abu Dhabi, UAE

<https://mbzuai.ac.ae/>

## Abstract

*The performance of the Deep Learning (DL) models depends on the quality of labels. In some areas, the involvement of human annotators may lead to noise in the data. When these corrupted labels are blindly regarded as the ground truth (GT), DL models suffer from performance deficiency. This paper presents a method that aims to learn a confident model in the presence of noisy labels. This is done in conjunction with estimating the uncertainty of multiple annotators. We robustly estimate the predictions given only the noisy labels by adding entropy or information-based regularizer to the classifier network. We conduct our experiments on a noisy version of MNIST, CIFAR-10, and FMNIST datasets. Our empirical results demonstrate the robustness of our method as it outperforms or performs comparably to other state-of-the-art (SOTA) methods. In addition, we evaluated the proposed method on the curated dataset, where the noise type and level of various annotators depend on the input image style. We show that our approach performs well and is adept at learning annotators' confusion. Moreover, we demonstrate how our model is more confident in predicting GT than other baselines. Finally, we assess our approach for segmentation problem and showcase its effectiveness with experiments.*

## 1. Introduction

Real world data is replete with noisy labels. Since the labeling process of large-scale datasets is costly and time-consuming, researchers often resort to less expensive options, such as internet inquiries and crowdsourcing to circumvent this issue [32, 38]. Unfortunately, these methods are viable in producing datasets with incorrect labels. Smaller datasets are also vulnerable to the presence of corrupted labels. In

this case, usually the labelling process is either challenging or the annotators have divergent opinions [3, 21]. In medical imaging, for example, it is imperative to procure annotations from the clinical experts. However, it is not only expensive to obtain annotated data, but it also suffers from high inter-reader variability among domain's experts [17, 20].

Deep Neural Networks (DNN) noticeably suffer a degeneration in performance when trained on noisy labels. To combat this issue, various algorithms have been devised to adapt to the presence of noisy labels without compromising on the performance of DNNs. Sample Selection methods [10, 12, 22, 34, 40] started to gain momentum recently; these methods involve a two network, Student-Teacher, for learning from noisy labels. It uses a small loss trick to sample clean instances for additional training by its peer network. While these methods aid in selecting the clean samples, the small loss trick does not perform well when the loss distribution of true-labelled and false-labelled examples overlap substantially.

In the instance when there is a significant level of dispute in the labels by the annotators, conventional training methods that consider such labels as "the truth" result in models with low predictive ability. Tanno et al [31] proposed an algorithm that jointly estimates the annotators' confusion and the underlying label distribution. The annotators' confusion is represented by a stochastic transition probability matrix. In their approach, the loss function is augmented by adding a regularization term that is the trace of annotators' confusion matrix. However, the caveat is that this regularization may still penalize in instances when the annotator is not confused, therefore it will not learn the true annotator's noise distribution. Furthermore, there is no incentive in the training process to enforce the classifier network to predict the class probabilities.

Our work is inspired by [31, 41], with a motivation to make our model confident in its predictions while also jointly

estimating annotator’s confusion in the presence of noisy labels. We explored entropy and information regularizer techniques to encourage our classifier to make confident predictions about each class.

**Problem Statement.** In this paper, we focus on supervised learning problem with noisy labels. We assume that each object  $x_n$ ,  $n = 1, \dots, N$  is assigned with a set of noisy labels  $\{\tilde{y}_n^{(r)}\}_{r=1}^R$ , where  $\tilde{y}_n^{(r)}$  is a label given to the object  $x_n$  by annotator  $R$ . Here  $N$  denotes the total number of samples in the data, and  $R$  denotes the total number of annotators. The main goal is to construct an algorithm that learns the distribution of true labels  $p(y|x)$  and to make confident predictions about the classes. This is achieved in conjunction with estimating annotator’s noise.

To achieve this, we use the classifier-annotator approach [31]. We jointly train two neural networks: classifier and annotator. The first network, the classifier, aims to learn the ground truth/class true label. So it outputs the class probability vector  $\hat{p}_\theta(x)$ . The second network learns each annotator’s confusion matrix  $U(x)$ , which represents the likelihood of the annotator being wrong in the class markup for a given input.

However, it is not enough to minimize the loss between matrix-vector product  $\hat{U}_\psi(x)\hat{p}_\theta(x)$  and annotator’s label  $\tilde{y}$  due to various reasons. First of all, there is no evidence why annotator and classifier neural networks will learn confusion matrix and class probabilities. There are infinite number of pairs  $(\hat{U}_\psi(x), \hat{p}_\theta(x))$  that approximate  $\tilde{y}$  well. Without a modification of loss functions, it may turn out that they just learn some features of inputs. Secondly, we want to be confident in the predictions of the classifier. In evaluation mode, this model will be used to make real-time predictions. It is important to train the model in a such a way that it makes confident and true predictions.

To tackle the aforementioned problems, we penalize the classifier network for uncertainty. We propose two regularization techniques based on Shannon’s entropy and information. Our methodology for classification is summarized in Figure 1. Moreover, we apply our methodology for segmentation problem. In this case we make predictions and estimate the confusion pixel-wise.

**Contributions.** The main contributions of our paper are outlined as follows:

1. **Learning the ground truth label.** Our approach is capable of disentangling the GT from the annotation noise. We distinguish the noise through the usage of the annotator-classifier methodology. We enforce the classifier network to learn class probabilities, not some features of the input, by regularizing its output via Shannons’ entropy and information-based regularizer.
2. **Learning confident model.** Our choice of regularization technique is enforcing the classifier network to make convincing predictions about the respective classes. This

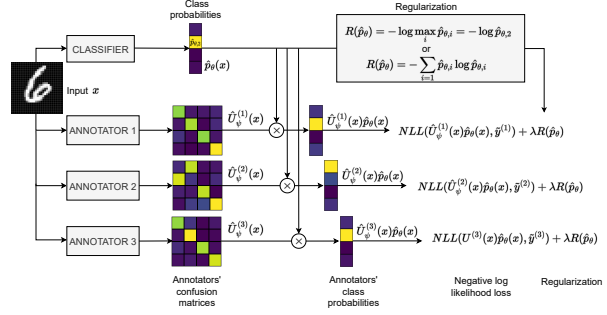


Figure 1. Model architecture. We consider the problem with 4 classes and 3 annotators. Architecture consists of two neural networks: 1) classifier network predicts class probabilities  $\hat{p}_\theta(x)$ , 2) annotator NNs predict confusion matrix  $U^{(r)}(x)$  for each annotator  $r$ . Matrix-vector product  $U^{(r)}(x)\hat{p}_\theta(x)$  estimates the annotator’s prediction. Note, that 2nd annotator tends to confuse classes 1 and 2. To jointly train two neural networks we minimize regularized negative log likelihood loss (NLL). We propose two options for regularization: information-based regularizer and entropy.

has various befitting practical applications in different domains, including medical imaging. We use our regularizer to push the predicted probabilities of the first network to be closer to 1 or 0 and to make the model to distinguish between classes better.

3. **Competitive numerical experiments.** We have performed extensive numerical experiments that compares our algorithm with other SOTA baselines. We conducted experiments on MNIST, CIFAR-10 and FMNIST datasets to gauge the performance of our algorithm in the existence of noisy labels. The noisy labels were simulated using pairflip and symmetric noise.

Our experiments showed that our algorithm outperforms all the evaluated baselines for the higher noise levels such as pairflip 45% and symmetric 50%. For smaller noise rates, we perform at par with [10, 31, 34, 35, 40]. Moreover, we show better results than in annotator-classifier setup with trace regularizer proposed in [30, 31]. Moreover, we conduct experiments for segmentation, where our model also shows better accuracy and confidence compared to trace regularization [41].

4. **Curated dataset.** We have also executed experiments for a curated dataset, where noise type and level for various annotators depend on input image style. The proposed approach with the choice of our regularizer results in more confident model compared to the one without the regularizer. Moreover, we show that our approach is able to learn true annotators’ confusion.

5. **Open code.** Our code is available online. Our implementation includes a suite that easily allows researchers to compare their approach against all benchmarks considered in this paper.

**Organization.** The remainder of the paper is organized as

follows. Related works are described in Section 2. Section 3 presents the methodology and probabilistic model behind it. In Section 4 we describe the proposed regularizers. Numerical experiments are provided in Section 5 (additional experiments are provided in Appendix C). Section 6 is dedicated to the segmentation problem, and concluding remarks and potential future research directions are given in Section 7.

## 2. Related Literature

Learning with noisy labelled training data has been an active area of research for some time. Various algorithms have been introduced and have shown resistance to noise during training. We highlight the core research being done in this domain.

### 2.1. Classification

**Noise Transition Matrix/Loss Correction.** Loss correction approach using noise transition matrix,  $T$ , is a crucial branch that is used in deep learning systems. The goal of loss correction is for training on noisy labels with the corrected loss to be roughly equivalent to training on clean labels with the original loss. The majority of the early approaches dealing with noisy labels relied on estimating a noise transition matrix to figure out how labels switch across classes.

Patrini et al. [25] introduced two different approaches for loss correction using a stochastic matrix  $T$  that delineates the probability of a class being flipped with another under a certain noise. This two loss correction approaches, namely, forward correction and backward correction. The backward procedure corrects the loss by multiplying the loss with inverse transition matrix  $T^{-1}$ ; while the forward procedure corrects the network predictions by multiplying it with  $T$ .

Hendrycks et al. [11] suggested Gold Loss Correction(GLC) based on Forward Correction to address extreme noise. The transition matrix cannot be accurately predicted by solely noisy data when there is significant noise present. The main driver is the assumption that a limited portion of the training data is reliable and accessible.

Sukhbaatar et al. [30] demonstrated a method of forward loss correction by introducing a stochastic matrix that quantifies label corruption, and cannot be calculated without accessing the true labels. In order to include learning about the label noise, forward loss correction involves adding a linear layer to the model’s end and adjusting the loss as necessary.

Through the use of soft and hard bootstrapping, Reed et al. added the concept of consistency to the prediction objective [26]. The soft version is identical to softmax regression with minimum entropy regularization, whereas the hard version adjusts regression targets by employing MAP estimation. This bootstrapping process, intuitively, gives the learner the opportunity to contest an inconsistent training label and re-label the training data to enhance the label quality. Whereas Goldberger et al. [9] made use of the

expectation-maximization (EM) algorithm to determine the optimal network and noise parameters. The use of transition matrices has been investigated further [4, 7, 36].

**Multi-Network Learning.** Multi-network training frequently employs collaborative learning and co-training. Therefore, the sample selection procedure is governed by the mentor network in the case of joint learning and the peer network in the case of co-training. These algorithms can be defined as learning to teach methods, and they comprise of a student and teacher network. The responsibility of the teacher network is to select more informative samples for enhanced student network training. Malach et al. proposed decoupling method that simultaneously trains two DNNs while only updating parameters on examples/samples in cases when the two classifiers disagree [22].

MentorNet [12] selects clean instances to guide the training of the student network after it has trained the teacher network first. Co-teaching [10] and [40] also employ two DNNs, but each DNN selects a certain number of small-loss examples and feeds them to its peer DNN for additional training. Co-teaching+ additionally utilize the disagreement strategy of Decouple. In comparison, JoCoR [34] reduces the diversity of two networks by means of co-regularization, making the predictions of the two networks more similar.

**Robust Regularization.** Tanno et al. [31] showcased a method for simultaneously learning the individual annotator model and the underlying true label distribution. Each annotator’s confusion is represented by a confusion matrix, which is estimated in conjunction with the classifier predictions. The algorithm comprised of a loss function include a trace regularization term. Menon et al. [23] suggests a composite loss-based gradient clipping for label noise robustness. It is expected that clipping would provide noise robustness, given that one does not place excessive trust in any single sample. Robust early-learning [35] distinguishes between critical and non-critical parameters for fitting clean and corrupted labels, respectively. Then, only non-critical updates are penalized with a different update rule.

**Other Deep Learning/Statistical Methods.** DivideMix [18] is a framework that splits the training data into a labeled set with clean samples and an unlabeled set with noisy samples-samples that comprise of noisy labels; it trains the model on both the labeled and unlabeled data in a semi-supervised approach. Kun Yi et al [39] proposed a probabilistic end-to-end noise correction in labels (PENCIL) framework. This method only uses noisy labels to initialize label distributions; the label distributions get updated by an iterative correction of the noisy labels. Consequently, label distributions are used in the calculation of the network loss instead of the noisy labels. Xia et al. [35] suggested a robust early-training method to diminish the side effect of noisy labels prior to early stopping. This helps with improving the memorization of clean labels. The parameters are

split into critical and non-critical parameters. Each of these parameters are updated with a different update rule.

## 2.2. Segmentation

Several strategies have been developed to solve the issue of annotator-related bias for segmentation in medical imaging. We review some prominent work in the field.

Inter-reader variability among annotators gave prominence to Simultaneous Truth and Performance level Estimation (STAPLE) [33] algorithm that uses expectation-maximization method to merge segmentations from various annotators into estimating a single ground truth. There are several algorithms that drew their inspiration from STAPLE framework such as [1, 2, 13, 14, 29]. These methods are reflective of generative modelling of annotator’s behaviour. Here the latent variables are the true labels which are unobserved, and the confidence/expertise of various annotators.

Mirikharaji et al. [24] provides a sample re-weighting strategy that considers the expertise level of annotators. This strategy gives greater weights in the loss function for the samples annotated by professionals. To disengage annotator bias, Tanno et al. [41] uses two coupled CNNs. Similar to [31], the CNN for segmentation estimates the label distribution, while the CNN for annotation is representative of the annotator bias using a confusion matrix.

Annotation distribution learning has been another active area that has inspired pioneer work of probabilistic U-Net (PU-NET) [15]. This method given an input, examines the problem of learning a distribution over segmentations. This proposed architecture is a generative segmentation model which is an integration of U-Net [27] and conditional variational autoencoders (VAE), and is effective in developing an extensive number of conceivable hypotheses/segmentation results.

## 3. Methodology

### 3.1. Probabilistic Model For Noisy Labels

Let  $\mathcal{X}$  denote the space that contains a set of input data  $X := \{x_1, \dots, x_n\}$ . Each of these objects  $x$  in the input data are assigned a corresponding label  $y$  such that  $Y := \{y_1, y_2, \dots, y_N\} \subseteq \mathcal{Y}$ , where  $\mathcal{Y}$  is the space of labels.

We synthetically induce noise in our original label set  $\mathcal{Y}$  to corrupt the clean labels. There are multiple different ways through which we create the noisy labels for our data, namely symmetric and pairflip noise types. In Section 5.1 and in the Appendix, we discuss in details about the mainstream noise types that we used to create noisy labels for the datasets that we utilized in this paper.

We denote the set of noisy labels given by annotator  $r$  that labels objects from the set  $X$  as  $\tilde{Y}^{(r)} = \{\tilde{y}_1^{(r)}, \dots, \tilde{y}_N^{(r)}\}$ , where  $r = 1, \dots, R$ . Our objective is to jointly estimate annotator noise as a function of input  $x$ , as well as to esti-

mate the distribution for latent GT label from noisy dataset,  $\mathcal{D} = \{X, \tilde{Y}^{(1)}, \dots, \tilde{Y}^{(R)}\}$ . In our architecture we add an entropy/information-based regularization term with the main loss function. The goal is to enforce our algorithm to make confident predictions while also learning the true labels. Following the strategy of [31, 41], we would now demonstrate how to set up a probabilistic model for data that has been annotated by multiple sources.

To model annotator-specific characteristics, there are some pivotal factors that are to be considered. In modelling multiple annotators, it is common to assume that annotators exercise their independence according to their expertise and experience in labelling an input data point  $x_i$ . The precision of annotator’s labeling may depend on the properties of the data point itself. Thus, we do not assume that annotators are equally competent (or incompetent) at labeling all the data; rather, it depends on the input they observe. This can be represented as a probabilistic model for random variables  $x$ ,  $y$ , and  $\tilde{y}$ . Following the work of [31, 38], we describe the joint conditional distribution of our probabilistic model as:

$$P(\tilde{Y}^{(r)}, Y|X) = \prod_{i=1}^N p(y_i|x_i) \prod_{r=1}^R p(\tilde{y}_i^{(r)}|x_i, y_i).$$

Here  $p(y_i|x_i)$  represents the distribution for the clean labels of the data samples. Conditional distribution  $p(\tilde{y}_i^{(r)}|x_i, y_i)$  signifies that the model estimates a noisy version of clean labels, represented as  $\tilde{y}_i^{(r)}$  for each annotator  $r$ . This makes intuitive sense as the noisy labels are not only conditional on true latent labels, but also on the input data. It is likely for the annotators to label some instances of data  $x_i$  with more precision than other samples. Since the annotators’ noise is dependent on the sample  $x$ , this allows us to model noisy label distribution as  $p(\tilde{y}^{(r)} = j|y = i, x) =: u_{j,i}^{(r)}(x)$ . We denote by  $U(x)$  a  $C \times C$  confusion matrix  $[U]_{j,i}(x) = u_{j,i}(x)$ , where  $C$  represents the number of classes for the true labels,  $y \in [1, \dots, C]$ . Now using the confusion  $U(x)$ , we can show the probability that input data  $x$ , labelled as  $i$  originally, is mislabelled as  $j$  in the set of noisy data:

$$\begin{aligned} p(\tilde{y} = j|x) &= \sum_{i=1}^C p(\tilde{y} = j|y = i, x) \cdot p(y = i|x) \\ &= \sum_i u_{j,i}(x) \cdot p(y = i|x). \end{aligned} \quad (1)$$

To represent the joint probability distribution of noisy labels using the confusion matrix of each annotator  $r$ , we can simplify (1) as:

$$p(\tilde{y}^{(1)}, \dots, \tilde{y}^{(R)}|x) = \prod_{r=1}^R \sum_{y=1}^C u_{\tilde{y}^{(r)}, y}^{(r)}(x) \cdot p(y|x).$$

### 3.2. Jointly Optimizing the two Networks to estimate the Ground Truth and Confusion

We minimize negative log-likelihood (NLL) to jointly optimize the parameters  $\theta$  and  $\psi$  of classification and annotator networks respectively. Given the data that

comprises of training inputs and noisy labels, we would minimize the negative log likelihood between the observed noisy labels and predictions from annotator label distribution as follows:  $-\log p(\tilde{Y}^{(1)}, \dots, \tilde{Y}^{(R)}|X) = \sum_{i=1}^N \sum_{r=1}^R \text{NLL}(\hat{U}_\psi^{(r)}(x_i)\hat{p}_\theta(x_i), \tilde{y}_i^{(r)})$ , where  $\hat{p}_\theta(x_i)$  is the output of the classification network and  $\hat{U}_\psi^{(r)}(x)$  is the output of annotator's  $r$  network. Minimizing this loss function alone can cause several problems. Firstly, it does not ensure that predictions of the classification network will be class probabilities. It can learn some feature of inputs in order to minimize the NLL loss between the pipeline output  $\hat{U}_\psi^{(r)}(x)\hat{p}_\theta(x)$  and corrupted labels  $\tilde{y}^{(r)}$ . Secondly, there is no guarantee that annotator matrices  $\hat{U}_\psi^{(r)}(x)$  are correctly learned to distinguish the noise from true labels. It can also learn some uninterpretable features of inputs  $x$ , such that  $\hat{U}_\psi^{(r)}(x)\hat{p}_\theta(x)$  is close to  $\tilde{y}^{(r)}$ .

To tackle these problems, we would add a regularization term that is attached to the base classifier which helps in estimating the true class probabilities of the predicted ground truth. The main loss, NLL loss is then jointly optimized with a regularization  $R(\hat{p}_\theta(x))$ . We propose two options for regularization: entropy regularization  $R(p) = -\sum_i p_i(x) \log p_i(x)$  and information-based regularization  $R(p) = -\log \max_i(p_i)$ . The combined loss is then given as:

$$-\log p(\tilde{Y}^{(1)}, \dots, \tilde{Y}^{(R)}|X) = \sum_{i=1}^N \sum_{r=1}^R \text{NLL}(\hat{U}_\psi^{(r)}(x_i)\hat{p}_\theta(x_i), \tilde{y}_i^{(r)}) + \lambda \frac{1}{N} \sum_{i=1}^N R(\hat{p}_\theta(x_i)).$$

Our classification network helps with learning the features of our data and gives us an estimate of the ground truth. The outputs of this network are probabilities with dimension  $B \times C$ , where  $B$  is the batch-size and  $C$  is the number of classes. Ideally we desire that the predictions we get from the classifier network are forced to give us 1 for the most probable class and 0 elsewhere.

We take the sum of this regularization term for the number of batch samples and then multiply it with a regularization parameter  $\lambda$  and then taking its average for the batch samples.

## 4. Confident Regularization

In this section, we will explain in detail the motivation for the choice of our regularizer. We used entropy and information based regularizer with the first network to enhance the predictions of our model in learning the ground truth.

### 4.1. Entropy Regularizer

Entropy is regarded as a measure for gauging uncertainty. The higher the entropy, the more disordered the state. Shan-

non et al. [28] mathematically described entropy as:

$$R(p) := -\sum_i p_i \log p_i = \mathbb{E}[-\log p].$$

where  $p_i$  denotes the  $i$ -th class probability. It is to be noted that entropy is a feasible choice as it a smooth function. So when  $p_i$  is 0, the function is still differentiable, since  $0 \log 0 = \lim_{p_i \rightarrow 0} p_i \log p_i$ .

### 4.2. Information Regularizer

We evaluated our experiments on another regularizer which resembles the information part of entropy. The motivation behind using this regularizer is the same as the entropy regularizer mentioned in Section 4.1. This regularizer is expressed as :

$$R(p) = \min_i(-\log p_i). \quad (2)$$

This regularizer would also push the classifier to make confident predictions. The caveat in using this regularizer is that it becomes undefined when  $p_i = 0$ . To counter that, we modified the regularizer function to:

$$R(p) = -\log(\max_i p_i).$$

Also, we would show that we achieve similar results when we compare it with entropy regularizer. The advantage of using entropy regularizer is that it's a smooth function unlike (2).

### 4.3. Motivation for Confident Regularization

As we mentioned before, it is not enough to minimize the loss between  $\hat{U}_\psi(x)\hat{p}_\theta(x)$  and  $\tilde{y}$ . Indeed, let  $U$  be the true confusion of the annotator and  $P_\theta(x)$  the confusion matrix of classifier. Ideally, we want  $P_\theta(x) = I$  and  $\hat{U}_\psi(x) = U$ . However, there can be a lot of pairs  $(\hat{U}_\psi(x), P_\theta(x))$  that satisfy  $\hat{U}_\psi(x)\hat{p}_\theta(x) = U$ . Therefore, we add an entropy regularizer, to enforce  $P_\theta$  converge to  $I$ .

**Theorem 1.** *Assume that classifier is confident, i.e.  $\hat{p}_\theta = e_i$  if  $y = i$ , where  $e_i$  is a basis vector of  $i$ -th coordinate. Then, minimizing NLL loss between  $\hat{U}_\psi^{(r)}(x)\hat{p}_\theta(x)$  and  $\tilde{y}^{(r)}$  over  $\hat{U}_\psi^{(r)}(x)$  we get*

$$[\hat{U}_\psi^{(r)}(x)]_{i,j} = p(\tilde{y}^{(r)} = j | y = i, x).$$

In Tables 1, Table 2, and Table 3, we show the performance of our algorithm with entropy and information-based regularizers on CIFAR-10, MNIST, and FMNIST datasets for symmetric and pairflip noise types. The theoretical comparison between the two regularizers is further discussed in Appendix ??.

## 5. Classification Experiments

### 5.1. Implementation Details

In this section we describe implementation details. We used a convolutional neural network (CNN) as a classifier

model which estimates the ground truth. The predictions of the classifier network are multiplied to the outputs of a fully connected annotator network that learns the confusion of the noisy labels. True labels are never introduced to the model during training. In our experiments, we synthetically introduce noise to the training data; we chose various noise rates, such as 20%, 30%, 45% and 50%.

We evaluate the performance of our algorithm for the classifier network as this aids in estimating the GT via making confident predictions about the true class. We are particularly interested in the performance of the classifier, as in evaluation stage this network will be used separately to make predictions.

**Baselines.** We compare our algorithm with the following approaches: (i) Co-teaching [10], which simultaneously trains two DNN models, with each network selecting the batch of data for the other, based on the instances with a small loss. (ii) Co-teaching+ [40], also employs samples with small loss, but with disagreement about predictions. This is the selection criteria for the networks to pick data for each other. (iii) JoCoR [34], extends on the idea of [10, 40], but uses co-regularization to minimize the diversity of the two networks, thus bringing the predictions of the two networks closer together. (iv) Robust Early-learning (CDR) [35], categorizes the critical and non-critical parameters for clean and noisy label fitting, respectively. Different update rules are applied to update these parameters. (v) Annotator Confusion (Trace) [31] is a regularized approach that assumes the existence of various annotators to simultaneously learn the individual annotator model and the underlying true label distribution, using only noisy observations.

**Datasets.** We used the standard benchmark datasets: MNIST [8], FMNIST [37], and CIFAR-10 [16] to demonstrate the effectiveness of our methodology.

**Types of Noise.** The noise types, used in the experiments, are described below.

1. **Pairflip Noise.** The pairflip noise involves swapping the labels of two adjacent categories/classes based on a preset ratio. [19]
2. **Symmetric Noise.** In symmetric noise, a portion of the original labels are retained, while the remainder are uniformly reassigned to all other categories [21]. This noise type is intended to imitate the random noise in the actual world, which is typically the result of random web crawling or manual annotation errors. It does not consider the similarities between classes.

## 5.2. Comparison with State-Of-The-Arts

**Results on MNIST.** We used the same backbone architecture to compare our algorithm against the baselines. Table 1 shows the performance comparison of our algorithm with the other methods. We see that for a smaller noise rate such

as 20% and 30%, which is evidently the least challenging case, all algorithms seem to show comparable performance above 97% for both pairflip and symmetric noise. However, when noise rates increases to 45% or above, there seems to be a distinct contrast in the performance of other algorithms, as the accuracy of some methods visibly decline to below 90% in the case of pairflip noise. Our method achieves an accuracy of 99.10% for pairflip 45% noise using entropy regularizer, followed closely by the Trace method with an accuracy of 97.95%. Whereas Co-teaching, JoCoR and CDR achieves the test accuracy of 87.63%, 85.86% and 87.04% respectively. For symmetric-50% noise, we got test accuracy of 98.94% with information regularizer, with Trace and CDR following closely behind at 98.87% and 97.72% respectively. The results of the our methodology with entropy and information-based regularizers are comparable.

**Results on CIFAR-10.** Table 2 shows the test accuracy results on CIFAR-10 dataset. Our algorithm performs distinctly superior when noise gets extreme; we achieve 80.03% accuracy for symmetric 50% noise with information regularizer, surpassing all the baselines. For pairflip 45%, we distinctly outperform all the baselines by a considerable margin. We acquired an accuracy of 83.43%, which is about 8% better than Trace method. All the other baselines acquired accuracy of less than 70%. Hence, our algorithm clearly outperforms all the baselines. This reinforces that for higher noise ratios, our algorithm consistently gives better performance as entropy and information regularization strategy helps the model to be more certain in its predictions.

Our algorithm still surpasses in performance when the noise rate is small for symmetric and pairflip noise types. For symmetric noise 20% and 30%, we achieved an accuracy of 84.22% and 83.85% respectively. The other algorithms contested close for symmetric 20% noise by accomplishing a test accuracy of 82.86% for Trace, 82.82% for Co-teaching, 81.12% for JoCoR, 81.01% for CDR, and with Co-teaching+ settling with an accuracy of 79.51%.

In pairflip noise 20% and 30%, we again outperform other methods by accomplishing an accuracy of 84.92% and 84.5% in the given sequence. Here, CDR and Trace follow closely behind with an accuracy of 82.89% and 83.86% respectively for pairflip 20% noise. For pairflip 30%, CDR attained an accuracy of 82.08%, while Trace achieved 83.15%.

**Results on FMNIST.** The experimental results of our algorithm compared with other baselines is shown in Table 3. Our algorithm has shown robust performance across most baselines.

We see comparable performance among all the algorithms when the noise rate is 20% and 30% for both symmetric and pairflip noise types. We see distinguishing performance when the noise gets extreme.

At symmetric 50% noise, we perform about 12% better than Co-teaching+ algorithm, while we outperformed CDR

Table 1. Test accuracy (%) on *MNIST* dataset.

Noise rate	Ours-Inf	Ours-Ent	Co-tea.	Co-tea.+	JoCoR	Trace	CDR
symmetric 20%	99.20	<b>99.48</b>	99.01	98.88	98.82	99.16	98.97
symmetric 30%	<b>99.11</b>	99.09	98.78	98.38	98.40	99.01	98.75
symmetric 50%	<b>98.94</b>	98.93	92.24	95.26	96.83	98.87	97.72
pairflip 20%	99.08	<b>99.55</b>	98.84	98.59	98.89	99.13	98.88
pairflip 30%	98.94	<b>99.54</b>	98.57	97.95	98.56	99.08	98.50
pairflip 45%	98.77	<b>99.10</b>	87.63	71.36	85.86	97.95	87.04

Table 2. Test accuracy (%) on *CIFAR-10* dataset

Noise rate	Ours-Inf	Ours-Ent	Co-tea.	Co-tea.+	JoCoR	Trace	CDR
symmetric 20%	<b>84.22</b>	84.00	81.82	79.51	82.12	82.86	81.01
symmetric 30%	<b>83.85</b>	83.26	80.69	79.29	80.95	80.45	78.90
symmetric 50%	<b>80.03</b>	79.64	75.74	73.19	76.60	77.82	69.68
pairflip 20%	<b>84.92</b>	84.78	81.17	79.59	81.86	83.86	82.89
pairflip 30%	84.36	<b>84.54</b>	79.53	77.83	79.52	83.15	82.08
pairflip 45%	<b>83.43</b>	81.23	59.04	47.72	67.59	75.88	58.56

Table 3. Test accuracy (%) on *FMNIST* dataset.

Noise rate	Ours-Inf	Ours-Ent	Co-tea.	Co-tea.+	JoCoR	Trace	CDR
symmetric 20%	90.67	90.79	90.48	88.69	<b>91.88</b>	90.61	88.69
symmetric 30%	<b>91.35</b>	90.34	90.36	88.50	91.33	89.64	87.38
symmetric 50%	<b>89.51</b>	89.49	89.37	77.96	89.21	88.94	85.36
pairflip 20%	90.90	90.77	90.68	89.12	<b>91.37</b>	90.40	90.01
pairflip 30%	90.38	<b>90.65</b>	90.11	89.06	89.67	90.33	88.78
pairflip 45%	<b>89.37</b>	89.02	78.86	52.61	88.10	89.08	64.63

by about 4%. We surpassed other baselines by small margins for this instance of noise. For pairflip 45%, we performed significantly better than Co-teaching+ and CDR algorithms which achieved accuracy of 52.61% and 64.63% respectively. Trace algorithm comes second in performance with 89.08% accuracy, followed closely by JoCoR at 88.10%.

Two network architectures such as Co-teaching, Co-teaching+, and JoCoR suffers in performance when the noise level increase in both symmetric and pairflip noise types. Trace comes closer in comparison with our algorithm, but we outperform it in all experiments. Both entropy and information-based regularizers perform at par compared to each other.

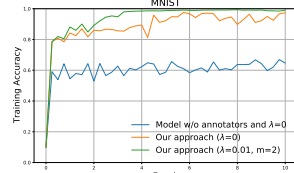
### 5.3. Curated Dataset

We have assembled the dataset that is based on *MNIST*, where noise level depends on input image style for various annotators. Three type of image styles were simulated by performing morphological transformations (in particular, thinning and thickening) on the original images, using Morpho-*MNIST* software [5]. In addition to the noise types described in Section 5.1, asymmetric and pairflip with permutation where applied. In the latter, the ordered label categories were first permuted randomly and labels of two adjacent categories after permutation were swapped based on a preset ratio. Asymmetric noise is a block matrix transformation, where a portion of original labels are retained and the remainder is uniformly reassigned to closest four categories. The type and level of noises applied to original labels are provided in Table 4.

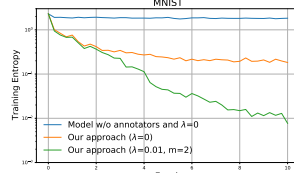
For a dataset consisting three different type of images (original, thin, and thick) and three different annotators (Table 4), we compare (i) classifier model without annotators and regularization, (ii) our approach without regularization,

Table 4. Annotator Information for three different styles (*MNIST*).

Annotators	Original	Thin	Thick
Annotator 1	symmetric 80%	asymmetric 40%	pairflip 95%
Annotator 2	pairflip with permutation 40%	symmetric 95%	asymmetric 70%
Annotator 3	pairflip 60%	pairflip with permutation 40%	symmetric 80%

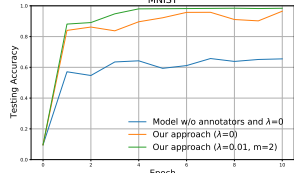


(a) Training accuracy

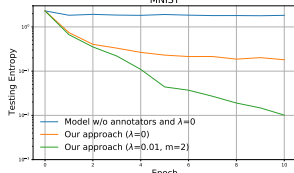


(b) Training entropy

Figure 2. Accuracy and entropy for Curated *MNIST* training data.



(a) Testing accuracy



(b) Testing entropy

Figure 3. Accuracy and Entropy for Curated *MNIST* testing data.

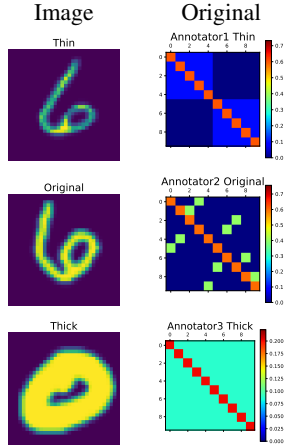


Figure 4. Original and Predicted confusion for different Annotators using different models: our approach with regularizer ( $\lambda = 2$ ,  $m=1.5$ ) and without it ( $\lambda = 0$ ). (*MNIST*).

and (iii) our approach with information-based regularization. Each annotator NN has similar architecture as in classifier model and takes images as an input. Everything else is the same as described in Section 3.

The result of experiments can be seen in Figures 2 and 3. Our approach is more accurate and confident compared to the classifier model. The accuracy of our approach with regularizer is higher and more confident than the model without the regularizer. This observation can be seen for both training and testing data. The proposed approach is able to learn the annotators' confusion. Predicted confusion matrices for each annotators and different image types are provided in

Table 5. Test DICE (%) and entropy evaluation on *MNIST* dataset for segmentation.

Metrics	Ours-Inf	Trace
DICE	96.97	96.62
Entropy	0.0453	0.0696

Figure 4. More results can be found in Appendix C.

## 6. Segmentation Experiments

We explored the performance of our algorithm with information-based regularization for segmentation. The whole approach is the same as for classification, but predictions would now be pixel-wise. Holistically, we followed the same idea in both the settings of classification and segmentation. The inputs of the model are the original images from MNIST with a Gaussian noise. Annotators (thin, thick, fractured) were simulated using morphological transformations [5] as mentioned in Section 5.3. The details for the MNIST segmentation dataset are provided in Appendix B.2.

For our method, we used the same model architecture as in [41], which is implemented as U-Net [27] with multiple output layers: the first is for prediction of true segmentation and the second is for predictions of noisy segmentations. We compared our method, which has information-based regularizer, with the trace-regularized approach [41].

## 6.1. Results

Table 5 shows the accuracy of the our method in comparison with the trace, and it also highlights the entropy calculated for these two methods. It can be seen that our model achieves better DICE similarity score and is more confident. Furthermore, in Figure 5, we visualised the results of the predictions for our method. It is clearly demonstrated that for an input image with Gaussian noise, our algorithm is able to produce excellent predictions about the true segmentation, with given annotators, as it matches closely the GT image.

## 7. Discussion & Conclusion

In this research, we proposed an approach of jointly training a two network model in a confident way. We improve classification/segmentation network by attaching regularization term (Information and Entropy) to make assured predictions. Moreover, our algorithm also learns annotators' noise and separate it from the true labels under extreme noisy supervision. We evaluated our algorithm on the standard datasets such as CIFAR-10, FMNIST and MNIST. In comparison with other state-of-the-arts, our method secured mature robust results. In classification task, we outperformed all baselines for extreme noise levels such as pairflip 45% and symmetric 50%. For smaller noise levels, we achieved

comparable performance with SOTAs. In segmentation problem, we achieved better DICE similarity score than [41]. We also show that prediction of classifier/segmentation model are more confident compared to other baselines. This demonstrates the effectiveness of our algorithm in making confident robust predictions about the true class labels/ground truth.

## References

- [1] Andrew J Asman and Bennett A Landman. Non-local statistical label fusion for multi-atlas segmentation. *Medical Image Analysis*, 17(2):194–208, 2013. 4
- [2] Landman BA Asman AJ. Robust statistical label fusion through consensus level, labeler accuracy, and truth estimation (collate). *IEEE transactions on medical imaging*, pages 1779–94, 10 2011. 4
- [3] Ella Barkan, Alon Hazan, and Vadim Ratner. Reduce discrepancy of human annotators in medical imaging by automatic visual comparison to similar cases, Feb. 9 2021. US Patent 10,916,343. 1
- [4] Alan Joseph Bekker and Jacob Goldberger. Training deep neural-networks based on unreliable labels. In *2016 IEEE International Conference on Acoustics, Speech and Signal Processing (ICASSP)*, pages 2682–2686, 2016. 3
- [5] Daniel Coelho Castro, Jeremy Tan, Bernhard Kainz, Ender Konukoglu, and Ben Glocker. Morpho-mnist: Quantitative assessment and diagnostics for representation learning. *CoRR*, abs/1809.10780, 2018. 7, 8
- [6] Daniel C. Castro, Jeremy Tan, Bernhard Kainz, Ender Konukoglu, and Ben Glocker. Morpho-MNIST: Quantitative assessment and diagnostics for representation learning. *Journal of Machine Learning Research*, 20(178), 2019. 11
- [7] Xinlei Chen and Abhinav Gupta. Webly supervised learning of convolutional networks, 2015. 3
- [8] Li Deng. The mnist database of handwritten digit images for machine learning research. *IEEE Signal Processing Magazine*, 29(6):141–142, 2012. 6
- [9] Jacob Goldberger and Ehud Ben-Reuven. Training deep neural-networks using a noise adaptation layer. In *ICLR*, 2017. 3
- [10] Bo Han, Quanming Yao, Xingrui Yu, Gang Niu, Miao Xu, Weihua Hu, Ivor W. Tsang, and Masashi Sugiyama. Co-teaching: Robust training of deep neural networks with extremely noisy labels. *Advances in Neural Information Processing Systems*, 2018-Decem(Nips):8527–8537, 2018. 1, 2, 3, 6
- [11] Dan Hendrycks, Mantas Mazeika, Duncan Wilson, and Kevin Gimpel. Using trusted data to train deep networks on labels corrupted by severe noise. *Advances in Neural Information Processing Systems*, 2018-December(Nips):10456–10465, 2018. 3
- [12] Lu Jiang, Zhengyuan Zhou, Thomas Leung, Li Jia Li, and Li Fei-Fei. Mentornet: Learning data-driven curriculum for very deep neural networks on corrupted labels. *35th International Conference on Machine Learning, ICML 2018*, 5:3601–3620, 2018. 1, 3

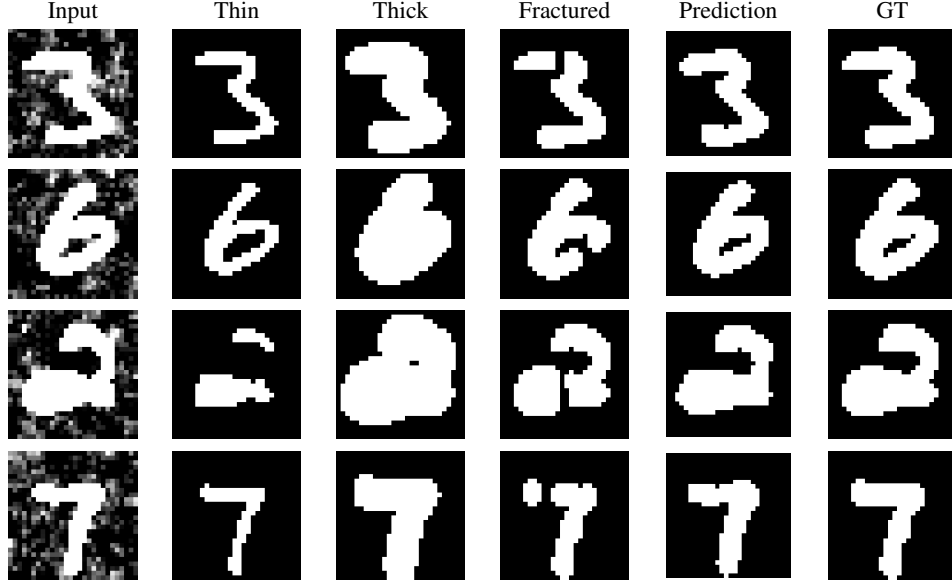


Figure 5. Visualisation of the predictions of the true segmentation along with the predictions of multiple annotators-Thin, Thick and Fractured using our algorithm in comparison with the test image and GT.

- [13] Modat M Jorge Cardoso M, Leung K. Steps: Similarity and truth estimation for propagated segmentations and its application to hippocampal segmentation and brain parcelation. *Medical image analysis*, 17:671–84, 02 2013. 4
- [14] Eytan Kats, Jacob Goldberger, and Hayit Greenspan. A Soft STAPLE Algorithm Combined with Anatomical Knowledge. *Lecture Notes in Computer Science (including subseries Lecture Notes in Artificial Intelligence and Lecture Notes in Bioinformatics)*, 11766 LNCS:510–517, 2019. 4
- [15] Simon A.A. Kohl, Bernardino Romera-Paredes, Clemens Meyer, Jeffrey De Fauw, Joseph R. Ledsam, Klaus H. Maier-Hein, S. M. Ali Eslami, Danilo Jimenez Rezende, and Olaf Ronneberger. A probabilistic U-net for segmentation of ambiguous images. *Advances in Neural Information Processing Systems*, 2018-December(NeurIPS):6965–6975, 2018. 4
- [16] Alex Krizhevsky. Learning multiple layers of features from tiny images. Technical report, 2009. 6
- [17] Elizabeth Lazarus, Martha B Mainiero, Barbara Schepps, Susan L Koelliker, and Linda S Livingston. Bi-rads lexicon for us and mammography: interobserver variability and positive predictive value. *Radiology*, 239(2):385–391, 2006. 1
- [18] Junnan Li, Richard Socher, and Steven CH Hoi. Dividemix: Learning with noisy labels as semi-supervised learning. *arXiv preprint arXiv:2002.07394*, 2020. 3
- [19] Xuefeng Liang, Xingyu Liu, and Longshan Yao. Review—A Survey of Learning from Noisy Labels. *ECS Sensors Plus*, 1(2):021401, 2022. 6
- [20] Geert Litjens, Thijs Kooi, Babak Ehteshami Bejnordi, Arnaud Arindra Adiyoso Setio, Francesco Ciompi, Mohsen Ghafoorian, Jeroen A.W.M. van der Laak, Bram van Ginneken, and Clara I. Sánchez. A survey on deep learning in medical image analysis. *Medical Image Analysis*, 42(1995):60–88, 2017. 1
- [21] Kede Ma, Xuelin Liu, Yuming Fang, and Eero P. Simoncelli. Blind image quality assessment by learning from multiple annotators. In *2019 IEEE International Conference on Image Processing (ICIP)*, pages 2344–2348, 2019. 1, 6
- [22] Eran Malach and Shai Shalev-Shwartz. Decoupling "when to update" from "how to update". *Advances in Neural Information Processing Systems*, 2017-Decem:961–971, 2017. 1, 3
- [23] Aditya Krishna Menon, Ankit Singh Rawat, Sashank J. Reddi, and Sanjiv Kumar. Can gradient clipping mitigate label noise? In *International Conference on Learning Representations*, 2020. 3
- [24] Zahra Mirikhrajji, Yiqi Yan, and Ghassan Hamarneh. Learning to segment skin lesions from noisy annotations, 2019. 4
- [25] Giorgio Patrini, Alessandro Rozza, Aditya Krishna Menon, Richard Nock, and Lizhen Qu. Making deep neural networks robust to label noise: A loss correction approach. *Proceedings - 30th IEEE Conference on Computer Vision and Pattern Recognition, CVPR 2017*, 2017-January:2233–2241, 2017. 3
- [26] Scott E. Reed, Honglak Lee, Dragomir Anguelov, Christian Szegedy, Dumitru Erhan, and Andrew Rabinovich. Training deep neural networks on noisy labels with bootstrapping. *3rd International Conference on Learning Representations, ICLR 2015 - Workshop Track Proceedings*, pages 1–11, 2015. 3
- [27] Olaf Ronneberger, Philipp Fischer, and Thomas Brox. U-net: Convolutional networks for biomedical image segmentation, 2015. 4, 8
- [28] Claude Elwood Shannon. A mathematical theory of communication. *The Bell system technical journal*, 27(3):379–423, 1948. 5
- [29] Ji Songbai, David W. Roberts, Hartov Alex, and Keith D. Paulsen. Combining Multiple Ture 3D Ultrasound Image

Volumes through Re-registration and Rasterization. *Med Image Comput Comput Assist Interv*, 23(7):903–921, 2005. 4

[30] Sainbayar Sukhbaatar, Joan Bruna, Manohar Paluri, Lubomir Bourdev, and Rob Fergus. Training convolutional networks with noisy labels. *3rd International Conference on Learning Representations, ICLR 2015 - Workshop Track Proceedings*, pages 1–11, 2015. 2, 3

[31] Ryutaro Tanno, Ardavan Saeedi, Swami Sankaranarayanan, Daniel C Alexander, and Nathan Silberman. Learning from noisy labels by regularized estimation of annotator confusion. In *Proceedings of the IEEE/CVF conference on computer vision and pattern recognition*, pages 11244–11253, 2019. 1, 2, 3, 4, 6

[32] Andreas Veit, Neil Alldrin, Gal Chechik, Ivan Krasin, Abhinav Gupta, and Serge Belongie. Learning from noisy large-scale datasets with minimal supervision. In *Proceedings of the IEEE conference on computer vision and pattern recognition*, pages 839–847, 2017. 1

[33] Simon Warfield, Kelly Zou, and William Wells. Simultaneous truth and performance level estimation (staple): An algorithm for the validation of image segmentation. *IEEE transactions on medical imaging*, 23:903–21, 08 2004. 4

[34] Hongxin Wei, Lei Feng, Xiangyu Chen, and Bo An. Combating Noisy Labels by Agreement: A Joint Training Method with Co-Regularization. *Proceedings of the IEEE Computer Society Conference on Computer Vision and Pattern Recognition*, pages 13723–13732, 2020. 1, 2, 3, 6

[35] Xiaobo Xia, Tongliang Liu, Bo Han, Chen Gong, Nannan Wang, Zongyuan Ge, and Yi Chang. Robust early-learning: Hindering the memorization of noisy labels. In *International conference on learning representations*, 2020. 2, 3, 6

[36] Xiaobo Xia, Tongliang Liu, Nannan Wang, Bo Han, Chen Gong, Gang Niu, and Masashi Sugiyama. Are Anchor Points Really Indispensable in Label-Noise Learning? In H Wallach, H Larochelle, A Beygelzimer, F d’Alché-Buc, E Fox, and R Garnett, editors, *Advances in Neural Information Processing Systems*, volume 32. Curran Associates, Inc., 2019. 3

[37] Han Xiao, Kashif Rasul, and Roland Vollgraf. Fashion-mnist: a novel image dataset for benchmarking machine learning algorithms. *arXiv preprint arXiv:1708.07747*, 2017. 6

[38] Yan Yan, Rómer Rosales, Glenn Fung, Ramanathan Subramanian, and Jennifer Dy. Learning from multiple annotators with varying expertise. *Machine Learning*, 95(3):291–327, 2014. 1, 4

[39] Kun Yi and Jianxin Wu. Probabilistic end-to-end noise correction for learning with noisy labels. *Proceedings of the IEEE Computer Society Conference on Computer Vision and Pattern Recognition*, 2019-June:7010–7018, 2019. 3

[40] Xingrui Yu, Bo Han, Jiangchao Yao, Gang Niu, Ivor W. Tsang, and Masashi Sugiyama. How does disagreement help generalization against label corruption? *36th International Conference on Machine Learning, ICML 2019*, 2019-June:12407–12417, 2019. 1, 2, 3, 6

[41] Le Zhang, Ryutaro Tanno, Mou Cheng Xu, Chen Jin, Joseph Jacob, Olga Ciccarelli, Frederik Barkhof, and Daniel C. Alexander. Disentangling human error from the ground truth in segmentation of medical images. *Advances in Neural Information Processing Systems*, 2020-Decem(NeurIPS):1–13, 2020. 1, 2, 4, 8, 11

## A. Proof of Theorem 1

*Proof.* Given samples  $x, y = i$  we want to minimize

$$\begin{aligned} & \frac{1}{R} \sum_{r=1}^R \mathbb{E}_{\tilde{y}|x,y} \left[ l(\hat{U}_\psi^{(r)}(x)p_\theta(x), \tilde{y}) \right] \\ &= \frac{1}{R} \sum_{r=1}^R \sum_{j=1}^C p(\tilde{y} = j|x, y = i) l(\hat{U}_\psi^{(r)}(x)e_i, \tilde{y}) \\ &= -\frac{1}{R} \sum_{r=1}^R \sum_{j=1}^C p(\tilde{y} = j|x, y = i) \log \frac{[\hat{U}_\psi^{(r)}(x)]_{j,i}}{\sum_{j=1}^C [\hat{U}_\psi^{(r)}(x)]_{j,i}} \end{aligned}$$

w.r.t.  $\hat{U}_\psi^{(r)}(x)$ ,  $r = 1, \dots, R$ . Since  $\hat{U}_\psi^{(r)}(x)$  is a stochastic matrix, we have  $\sum_{j=1}^C [\hat{U}_\psi^{(r)}(x)]_{j,i} = 1$ . Taking the derivative over  $[\hat{U}_\psi^{(r)}(x)]_{j,i}$ , we get

$$[\hat{U}_\psi^{(r)}(x)]_{j,i} = p(\tilde{y} = j|x, y = i). \quad \square$$

## B. Experimental Details

### B.1. Classification Datasets

**MNIST:** dataset comprise of 60,000 samples for training, and 10,000 data samples reserved for testing. The number of classes in the dataset is 10.

**CIFAR-10:** The CIFAR-10 dataset contains 60,000 color images in 10 classifications, with 6000 images each class. There are 50,000 training and 10,000 test images. The dataset is divided into five training batches and one test batch, each contains 10,000 images. The test batch is a collection of exactly 1,000 data samples randomly selected from each class. The training batches comprise of the remaining images in a random order, however it's likely that certain training batches may have more images from one class than another.

**FMNIST:** Fashion-MNIST is a dataset of article images from Zalando. It consists of a training set of 60,000 instances and a test set of 10,000 instances. Each instance is a  $28 \times 28$  grayscale image with a label from one of ten classes.

### B.2. Segmentation Datasets

**MNIST.** We also use the dataset used by [41]; synthetic noisy annotations were created based on the assumed GT to demonstrate the effectiveness of the method in a hypothetical setting where the GT is known. We apply the morphological alterations (such as thinning, thickening, fractures, etc.) to the ground-truth (GT) segmentation labels using the Morpho-MNIST software [6], we mimic a group of five annotators with a variety of distinguishing features/transformations. In particular, the first annotator near accurately segments the image ("good-segmentation"), and look similar to the GT. The second tends to over-segment ("thick-segmentation"), the third tends to under-segment ("thin-segmentation"), the

fourth is prone to a combination of over-segmentation and small fractures ("fracture-segmentation").

In a multi-class scenario, we first select a target class and then perform morphological operations on the provided GT mask to produce 4 different types of synthetic noisy labels: over-segmentation, under-segmentation, fracture segmentation, and good segmentation. Through the use of simulated annotators, we derive labels to create training data. However, the good segmentation remain remain latent and are not included during training of our algorithm.

### B.3. Types of Noise

Figure 6 shows the an example of noise transition matrices for pairflip 20% and symmetric 50% noise types. In addition, Figure 7 signifies the noise labels distributions for CIFAR-10 dataset for pairflip 45% and symmetric 50% noise types; this distribution of the label noise is used in the training process.

### B.4. Fine-tuning/Training

In this section, we would now further elaborate on the experimental details for each dataset that we used to validate our algorithm against.

**MNIST.** We used a LeNet model as a classifier for our backbone network. For the annotator network, we have a linear layer of size  $C \times C$ ,  $C$  denotes the number of classes. This linear layer represents our annotator confusion matrices, and we apply a softmax layer to it to make it a stochastic matrix along a certain dimension. We fine-tuned our model for a combination of learning rates,  $\alpha = [0.01, 0.001, 0.0001, 0.00001, 0.0016, 0.008, 0.0064, 0.005]$ , and about 50 different lambda values,  $\lambda$ , for our regularizer hyper-parameter. We started with a very small value of  $\lambda = 0.001506746$ , and slowly increased it exponentially (geometric progression) per epoch with a rate,  $r = 1.18$ ; we trained the model for 70 epochs and used Adam as an optimizer. In addition, the experiments were regulated to assess the performance of the model when the confusion matrix is initialized as an identity. These fine-tunings are done across all 2 different types of noise described in Section 5.1 with the respective noise rate that is associated with each of the noise types.

**CIFAR-10.** For CIFAR-10, we used ResNet-18 as our backbone network for the classifier. The annotator network remains unchanged (still has one linear layer that represents the confusion matrices of class  $C \times C$  that are stochastic). For this dataset, we fine-tuned the model for an assortment of learning rates, such as  $\alpha = [0.001, 0.00064, 0.0016, 0.00001, 0.005, 0.008, 0.0016, 0.00064]$ . We ran the model for 150 epochs; the hyperparameter  $\lambda$  for our regularizer was slowly increased exponentially again with a rate,  $r = 1.11$ .

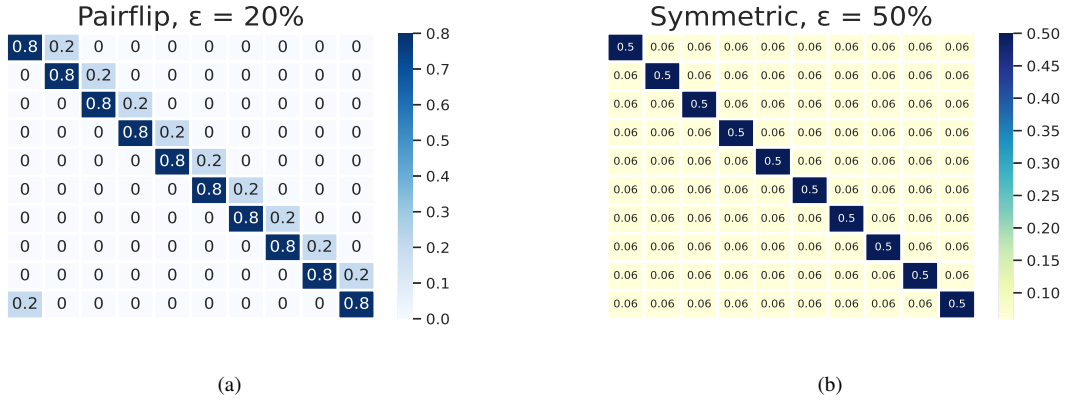


Figure 6. Noise Transition matrices for Pairflip and Symmetric noise.

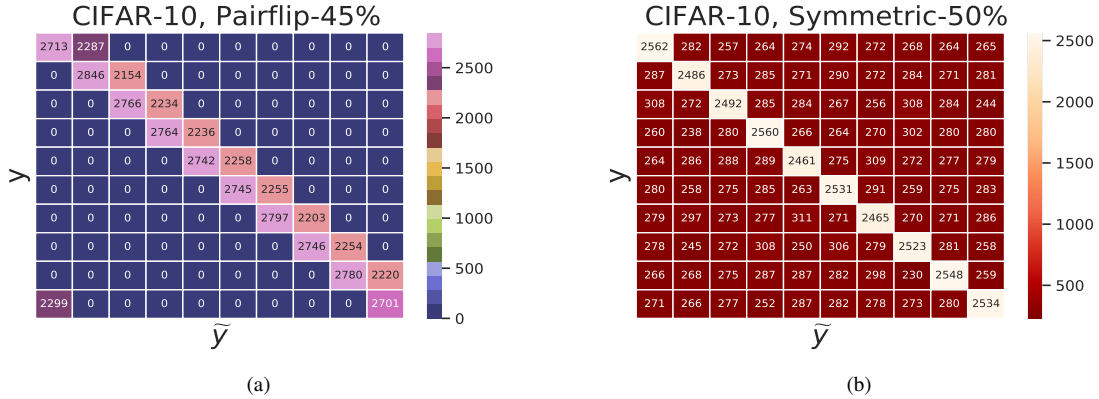


Figure 7. Confusion matrix between clean ( $y$ ) and noisy labels ( $\tilde{y}$ ) of CIFAR-10 dataset for (a) Pairflip-45% and (b) Symmetric-50% noise.

However, the starting value this time is  $\lambda = 3.0517578125e-05$ . We used a standard batch-size,  $BS=128$ . We used the standard augmentations of random crop of size  $32 \times 32$  and horizontal random flipping. These are the standard augmentations that have been used across all the baselines that we have evaluated. The remaining settings remain the same as described in MNIST above.

**FMNIST.** We kept the same settings of CIFAR-10, such as ResNet-18 model and batch-size of 128 for FMNIST dataset. The model was again fine-tuned for the same set of hyperparameters. However, the starting value of  $\lambda = 6.103515625e-05$ , and it was increased exponentially with a rate of  $r=1.12$ . We also retained the same set of augmentations that we used in CIFAR-10 dataset.

## C. Additional experimental results

In our earlier experiments, we kept the same type of noise and noise levels across all the number of annotators in the annotator network. This is usually not representative of the noise in the real world data, as it is possible that each

annotator would be independent in the way it is confused about labelling and annotating the data (subject to their own biases). Therefore, we confuse each annotator with different types and levels of noise. Table 6 shows the test accuracy of the classifier network on CIFAR-10, FMNIST and MNIST datasets for different types of noise for each annotators. We achieved comparable results with an accuracy of 84.12%, 91.12% and 98.97% for CIFAR-10, FMNIST and MNIST respectively. It's particularly notable that the accuracy of the classifier network remains at par even with using high level noise, such as pairflip 45% and symmetric 50% for two of the three annotators.

Table 6. Test accuracy (%) with three different annotators (Annotator1: Pairflip 45%, Annotator2: Symmetric 20%, Annotator3: 50%) representing different noise types and noise levels on CIFAR-10, FMNIST and MNIST datasets.

CIFAR-10	FMNIST	MNIST
84.12	91.62	98.97

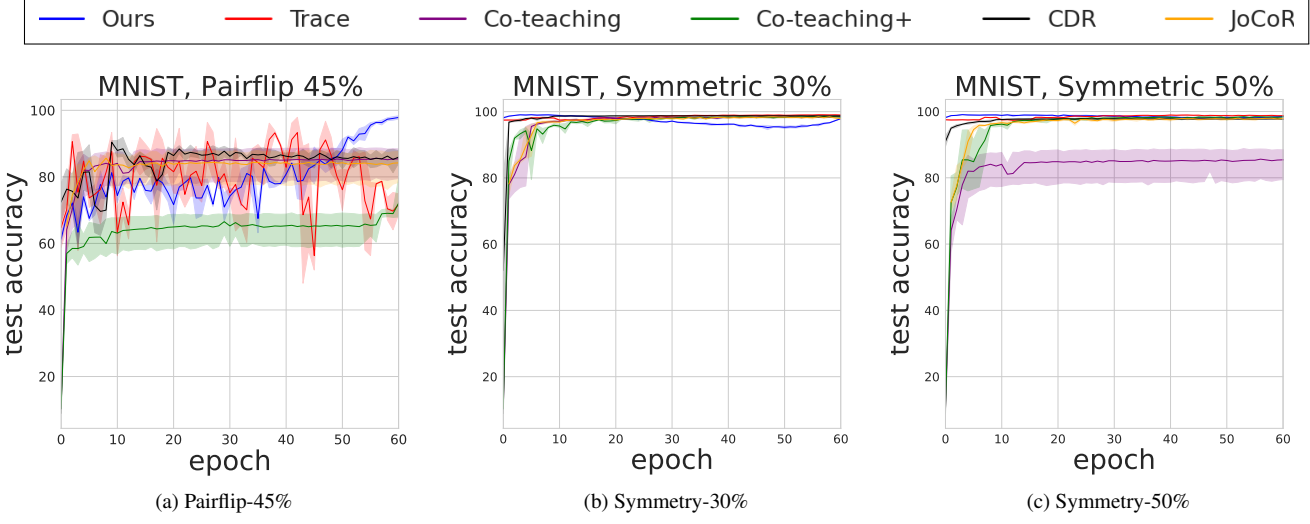


Figure 8. Test accuracy (%) vs. number of epochs on *MNIST* dataset.

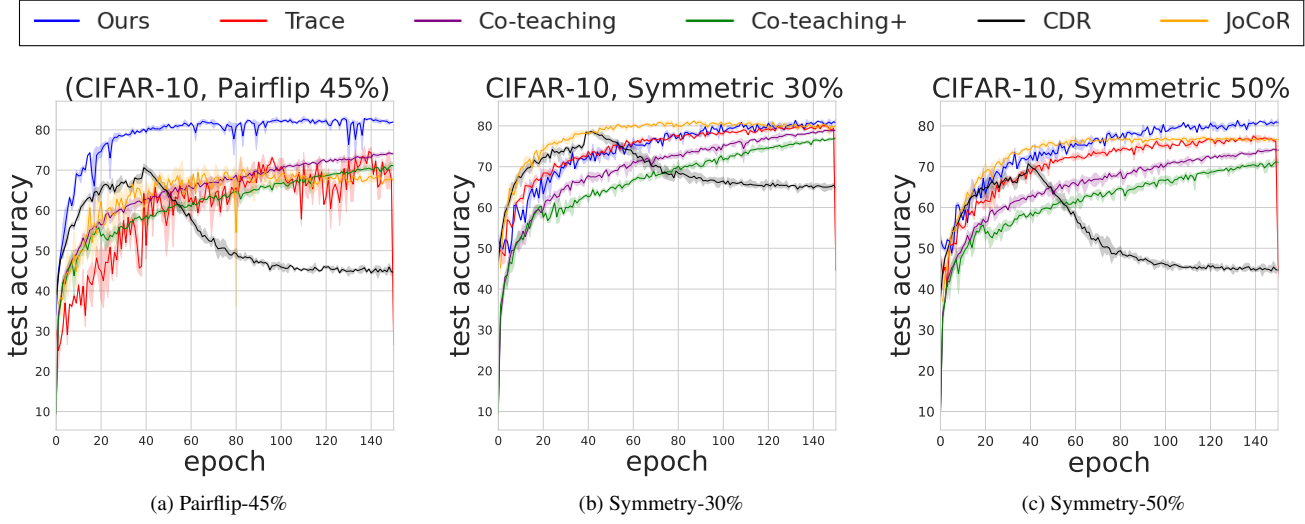


Figure 9. Test accuracy (%) vs. epochs on *CIFAR-10* dataset.

**MNIST** In Figure 8, we highlight the test accuracy vs. number of epochs. We can see clearly that for symmetric noise types, all algorithms gave comparable performance. It can be clearly seen that for symmetric noise, our test accuracy starts to decline a bit. This could be alleviated with an early stopping criteria which was not incorporated in these experiments. For pairflip 45%, the test accuracy starts to increase and stabilize in the later epochs of the experiment and transcends all the baselines.

**CIFAR-10** Figure 9 shows the illustrative results of test accuracy vs. number of epochs. In all the three plots, it can be clearly seen that our algorithm performs at par with the other algorithms, but the performance gets robustly superior

in the extreme noise type of pairflip 45%. This shows that our method is particularly robust again harder noise as it is able to make confident predictions.

**FMNIST** Figure 10 gives an illustrative result of test accuracy vs. number of epochs on FMNIST dataset. It showcases the test performance of our algorithm in comparison with other baselines. We can see that for all noise instances, our algorithm performs at par with the high achieving method like JoCoR. We perform considerably better against sample selection methods like Co-teaching and Co-teaching+, as well as against other method like CDR in the instance of pairflip 45%.

In addition, Figure 11 highlights the confusion matrices

of the true class and the predicted class by the classifier network of our algorithm. We show the confusion matrices plots for two extreme noise types pairflip 45% and symmetric 50% for all the datasets used. It is clearly seen that the confusion matrices are diagonally dominant thus highlighting the robust performance of our method.

**MNIST Curated Dataset** In Figure 12 we demonstrate annotators' confusion using our algorithm on the curated MNIST dataset that showcases different image styles of Original, Thin and Thick. The strength of the regularizer,  $\lambda=0.01$ , is increased by the multiplicative scalar  $m=2$  every epoch. Figures 13, 14 and 15 highlights the original and predicted confusion of annotator 1, annotator 2 and annotator 3 using our approach with the regularizer and the non-regularized approach (that is, when  $\lambda=0$ ).

**MNIST Segmentation** In Figure 16, the results of the annotators' (Thin, Thick and Fractured) predictions are visualised for our algorithm. The results demonstrate that our algorithm has produced good prediction results for the annotators.

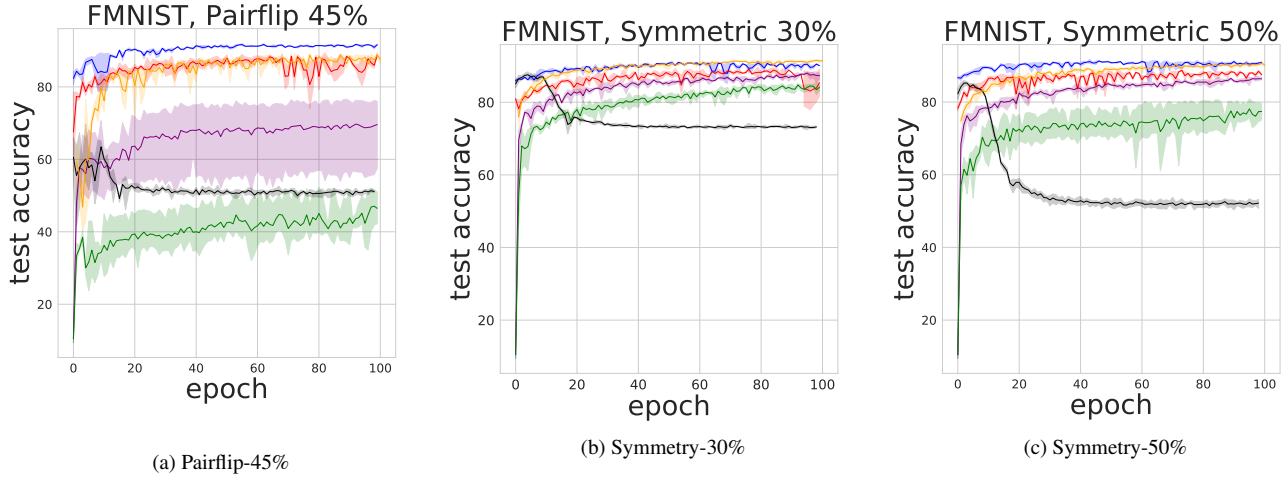


Figure 10. Results of test accuracy vs. number of epochs on *FMNIST* dataset.

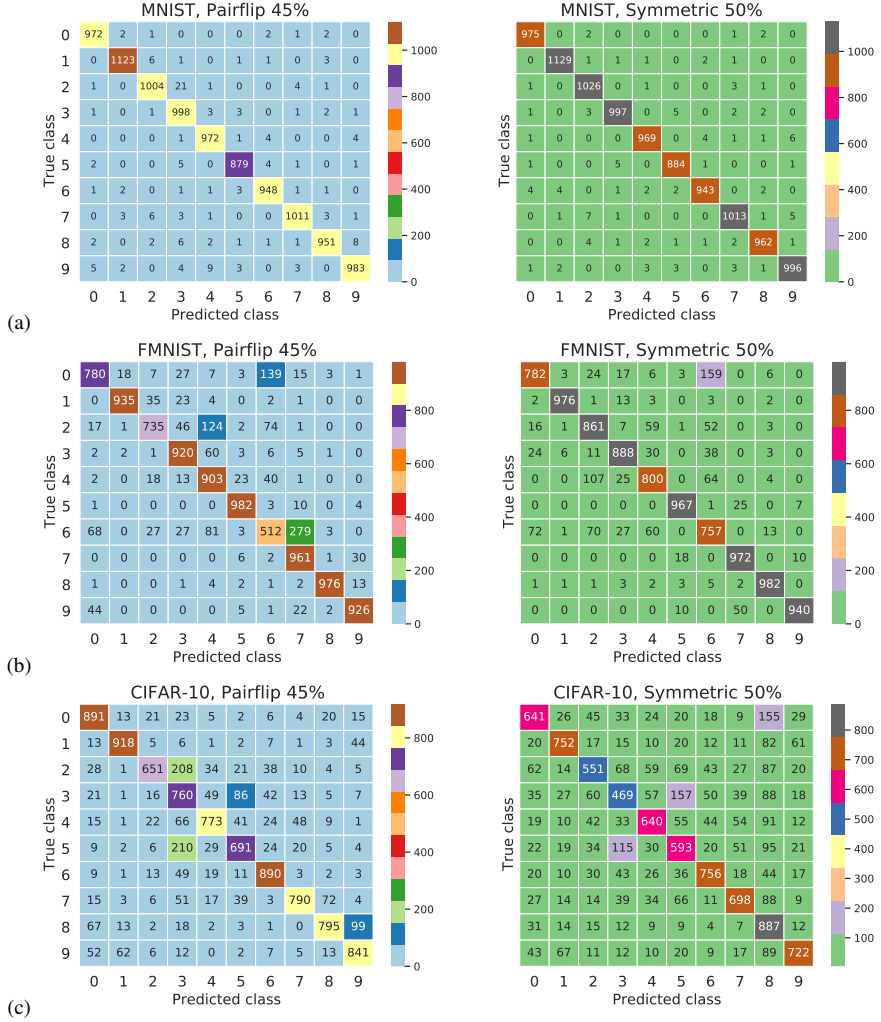


Figure 11. Confusion matrices of true class and predicted class for our algorithm for *CIFAR-10*, *MNIST* and *FMNIST* datasets.

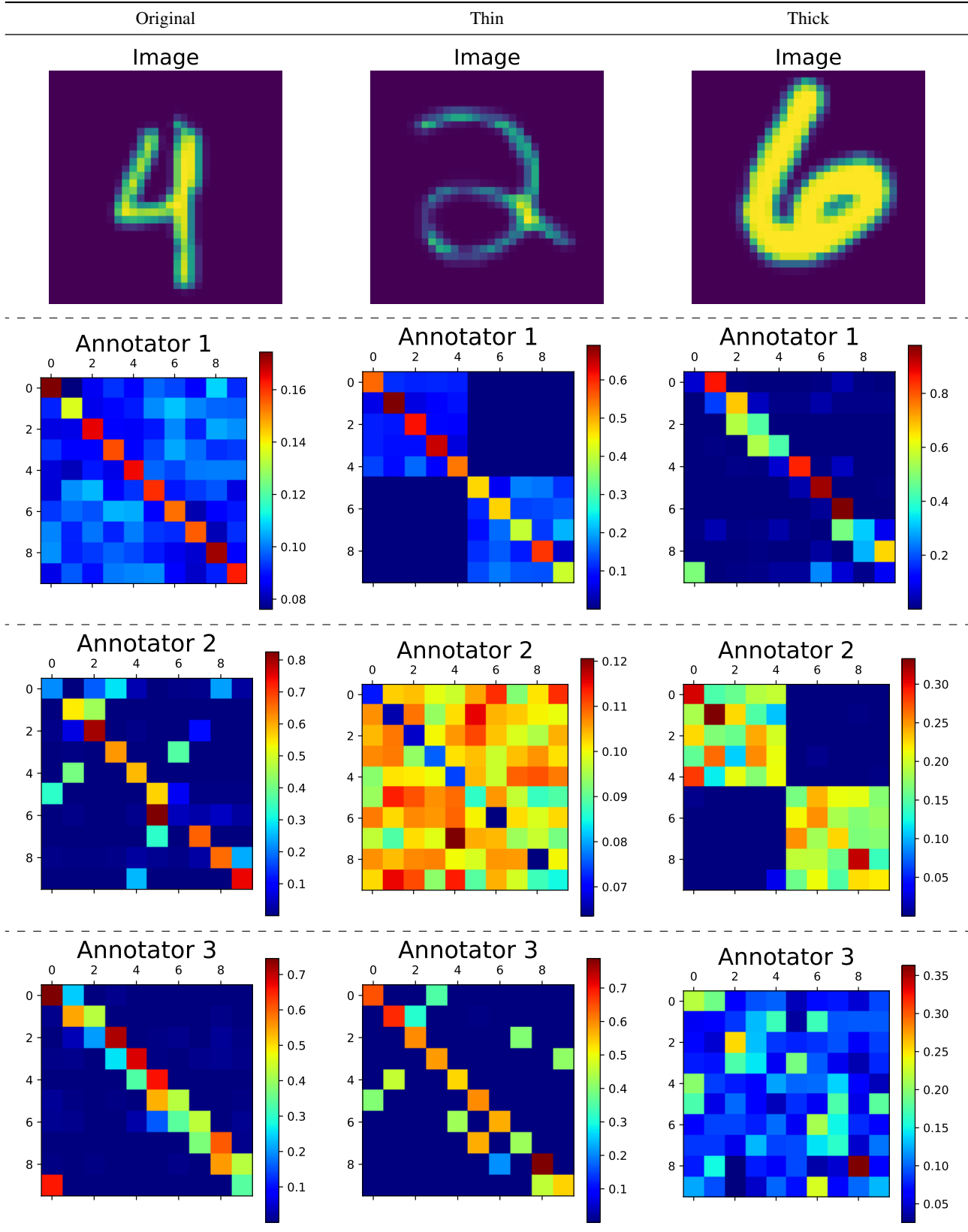


Figure 12. Learned Annotators' confusion for different image styles using our approach with the regularizer ( $\lambda=0.01$ ,  $m=2$ ) on MNIST dataset.

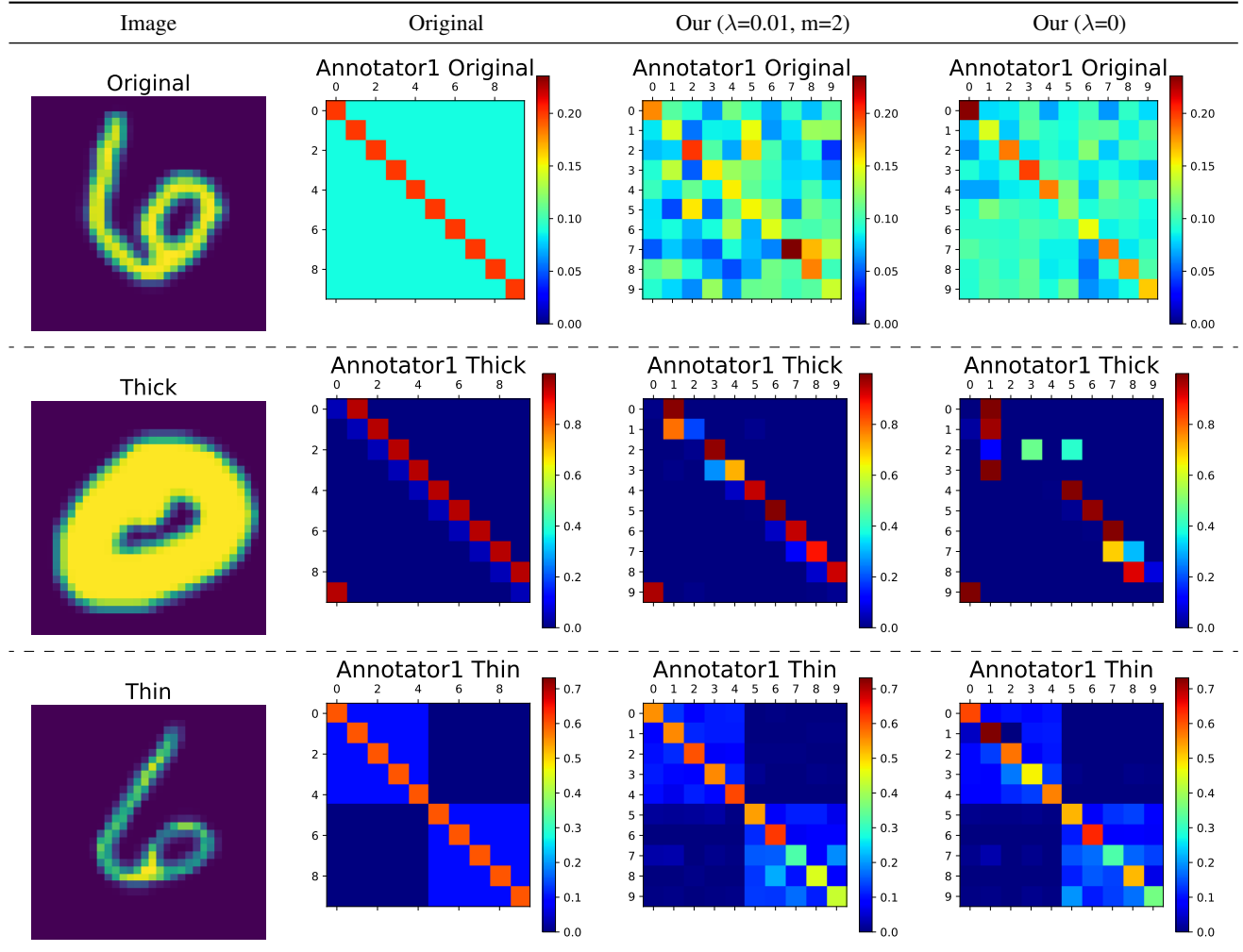


Figure 13. Original and Predicted confusion for Annotator 1 using different models: our approach with regularizer ( $\lambda = 0.01, m=2$ ) and without it ( $\lambda = 0$ ) on *MNIST* dataset.

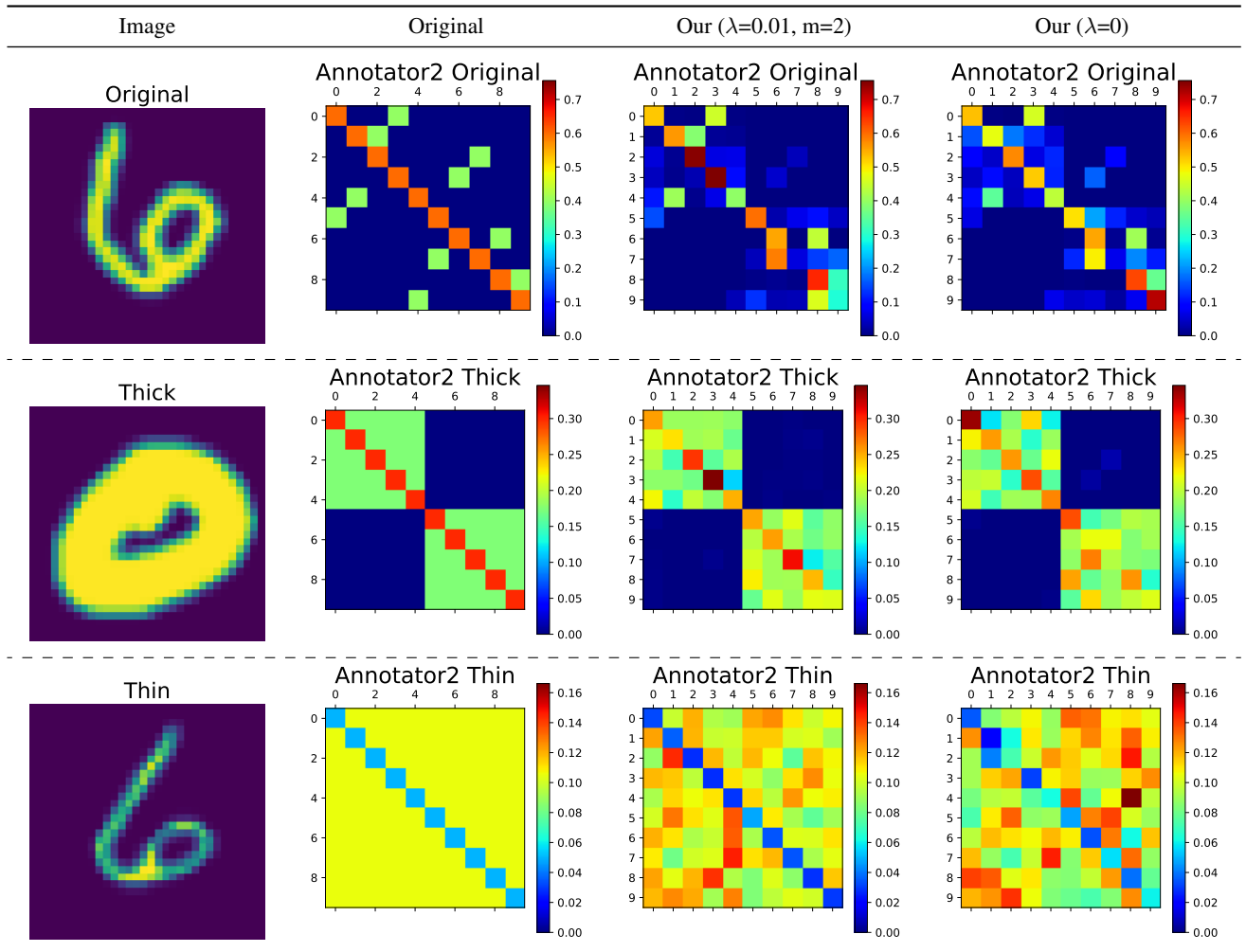


Figure 14. Original and Predicted confusion for Annotator 2 using different models: our approach with regularizer ( $\lambda = 0.01, m=2$ ) and without it ( $\lambda = 0$ ) on MNIST dataset.

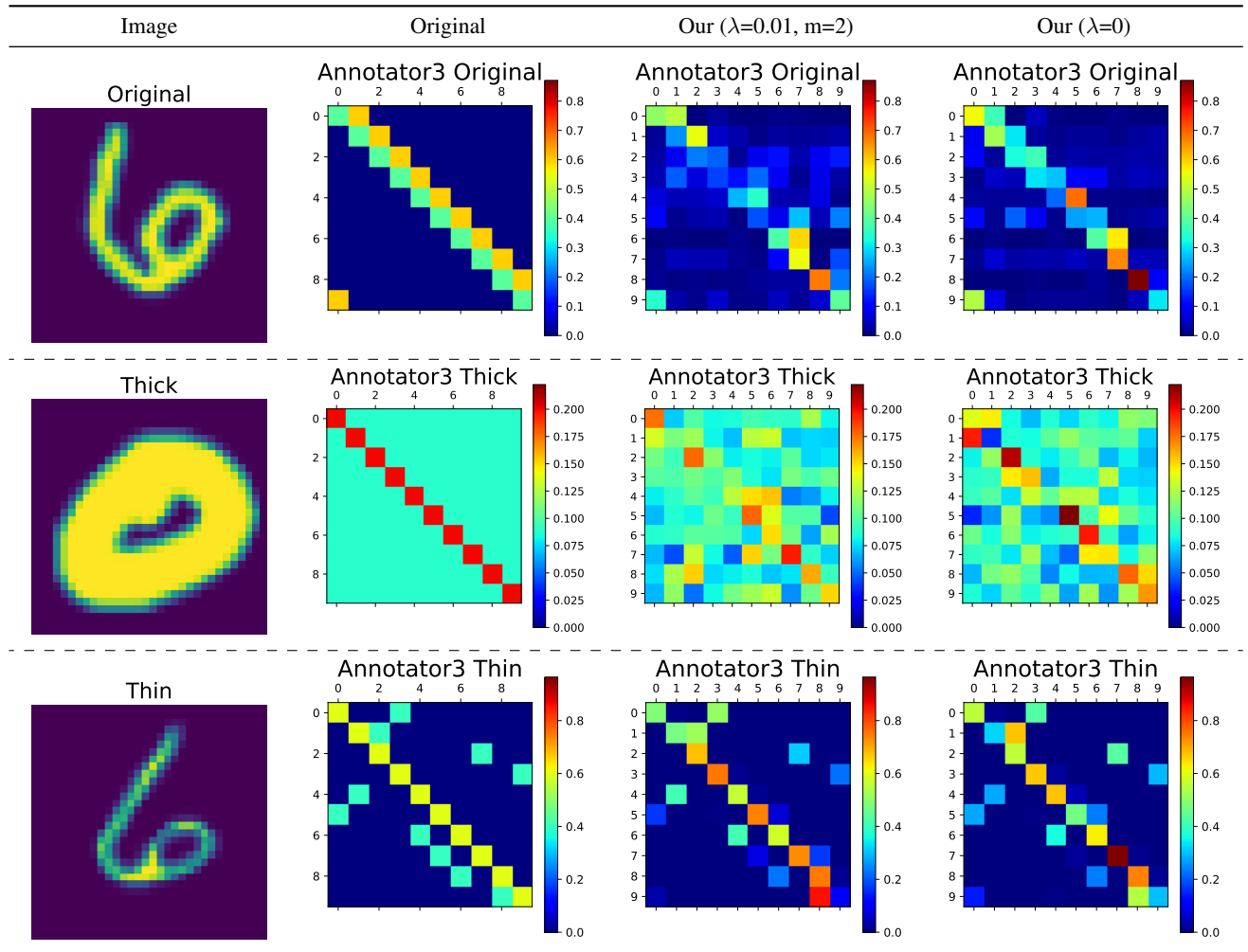


Figure 15. Original and Predicted confusion for Annotator 3 using different models: our approach with regularizer ( $\lambda = 0.01, m=2$ ) and without it ( $\lambda = 0$ ) on MNIST dataset.

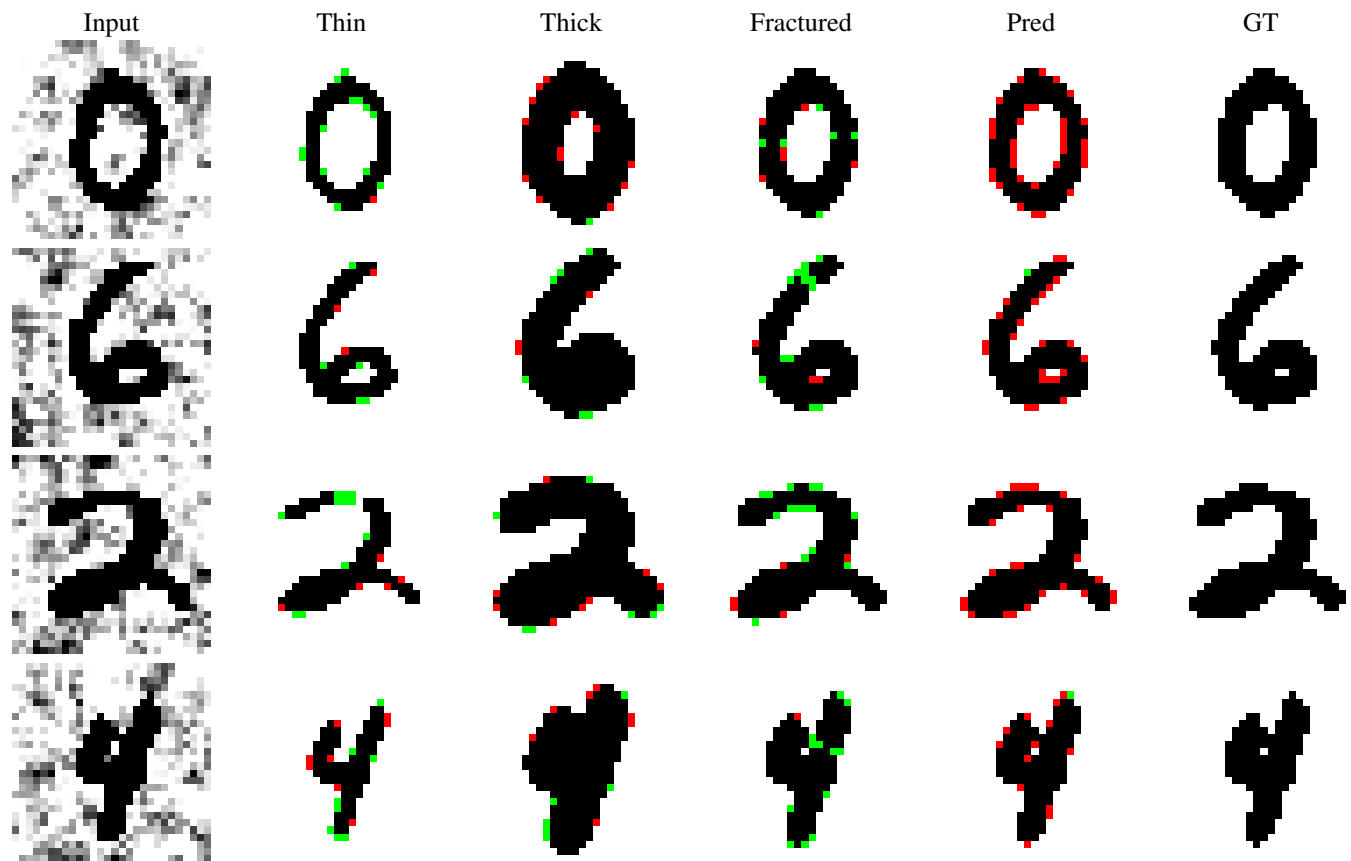


Figure 16. Visualisation of the predictions of the annotators' segmentations (Thin, Thick and Fractured) together with the predictions of the estimated true labels using our algorithm in comparison with the test image and GT. Black is true positive, White is true negative, Red represents false positive, whilst Green is false negative.